CRITICAL ANALYSIS OF LUNAR SURFACE FOR RETRIEVAL OF ITS PHYSICAL PROPERTIES: AN APPLICATION OF CHANDRYAAN – 1's MINISAR DATA. P. Mishra and D. Singh, Department of Electronics and Communication Engineering,Indian Institute of Technology Roorkee, Roorkee, India 247667. er.poojamisra@gmail.com, dharmfec@gmail.com

Introduction: MiniSAR onboard Chandrayan-1's mission is a hybrid polarimetric synthetic aperture radar operating at S-band (2.38 GHz). Stokes parameters (S_1, S_2, S_3, S_4) formed by using raw MiniSAR data {$|LH|^2$, $|LV|^2$, Re (LH LV*), Im (LH LV*)} are used to retrieve various child parameters, like circular polarization ratio (*CPR)*, Degree of polarization (*m*), etc [1]. Out of these parameter, CPR>1 is considered as the most important measure for finding water-ice deposits. However, this suggestion is hampered by the fact that surface roughness may also cause this behavior to occur [2]. Therefore, it is challenging to distinguish whether CPR>1 is caused due to surface roughness or due to water-ice deposits. In order to resolve this confusion, fractal dimension '*D*' has been measured [3,4] and an attempt has been made to distinguish two regions having *CPR*>1 due to water ice deposits or surface roughness by using fractal based approach which may be helpful in retrieving roughness information. For both of these regions, electrical and physical properties like real and imaginary part of dielectric constant [5,6], regolith bulk density [6,7], and loss tangent [6], have been retrieved.

*Fractal Dimension***:** For defining the roughness of any natural surface, fractal dimension '*D*' can be used because of its unique properties like, scale invariance and self similarity [3,4]. It defines the irregularity and roughness of any surface with its values lie in between 2.0 to 3.0. With increase in surface roughness, value of '*D*' increases. In this paper, local fractal dimension '*D*' has been measured with Triangular Prism Surface Area Method (TPSAM) for first Stokes vector (S_1) [8]. The effect of window size has also been observed on fractal dimension *D* by varying window size from 5×5 to window size 15×15. It has been observed that statistical parameters, like mean and standard deviation of *D* are constant (i.e., 2.15 and 0.1163) for window size 5 to 7. Then again, from window size 9 to 15, mean and standard deviation remain constant (i.e., 2.17 and 0.092). Due to small standard deviation in *D* values, window size 9 has been selected in this study [8]. Here, in this paper, D<2.17 has been selected as the criterion to obtain smooth regions.

Physical Properties: The real part of dielectric constant of lunar surface has been determined by using Campbell's approach [5],

$$\varepsilon' = \sin\varphi / \sin\left[\cos^{-1}\left(\frac{\sigma^0_{LH}}{\sigma^0_{LV}}\right)^{0.25} - \varphi\right] \quad (1)$$

where φ is the incidence angle of radar wave.

Bulk density of regolith can be determined as [7],

$$\rho_o = 3.53\log\varepsilon' \quad (2)$$

Loss tangent can be expressed as [6],

$$\tan\delta = 10^{(0.44\rho_0 - 2.943)} \quad (3)$$

Imaginary part of dielectric constant can be determined as,

$$\varepsilon'' = \varepsilon' \tan\delta \quad (4)$$

Theoretical Background and Methodology:

The CPR>1 signature may be caused either due to surface roughness or due to possible water-ice deposits. Thus, in this paper, an approach based on fusing the information of CPR and Fractal Dimension *D* has been proposed for studying the electrical properties of lunar surface.

This study has been performed on MiniSAR data of Peary crater which is large irregular shaped impact crater (diameter 77.7 km) located at 88.6° N, 33° E.

After obtaining regions with CPR>1, local fractal dimension '*D*' of first Stokes vector (S_1) is measured with TPSAM using window size 9×9 and *D* values have been observed in these regions. The local fractal dimension *D* may prove beneficial in accesing roughness information based on its values**.** Now, the criterion *D*<2.17 has been applied in order to segregate smooth regions from rough regions. Thus, regions with CPR>1 and *D*<2.17 (representing smooth regions) may have possibility of water-ice deposits, whereas regions having *CPR*>1 and *D*>2.17 may represent rough regions where CPR>1 is possibly occurring due to double-bounce effect takes place in rough blocky surface [9]. Thus, CPR>1 regions can be segregated in two parts:

i. Region 1: Probable icy regions : CPR>1, D<2.17
ii. Region 2: Rough blocky regions: CPR>1, D>2.17

For each of these regions, electrical properties described in (1)-(4) have been estimated.

Analysis:

The results of physical properties measured by (1)-(4) are presentented in Table-1. In order to examine the physical properties more elaborately six regions (ROIs) have been selected on the floor of Peary crater which are shown in Fig.1. The result of each electrical and physical parameter for these 6 regions are shown in Fig. 2-5. The results show that for each of the selected ROIs, the values of physical properties like ε', ε'', tanδ and ρ are less in region 1 than that of region 2 .

References: [1] Raney, R. K., (2007), IEEE TGRS, 45, 11, 3397-3404. [2] Spudis P.D. et al. (2010) GRL 37, L06204, doi:10.1029/2009GL042259. [3] Pant, T., et al. (2010), TGNHR, 1, 3, 243-257. [4] Pentaland, A. P., (1984), IEEE TPAMI, 6, 661-674. [5] Campbell B.A., et al.(2002), LPS XXXIII, Abstract #1616. [6] ZhenZhan, W., (2010), Science China, 53, 9, 1356-1378. [7] Olhoeft, G. R. and Strangway, D. W., (1975), Earth Planet Sci Lett., 24, 394-404. [8] Mishra, P., et al., (2013), IGARSS. [9] Campbell, D. B., et al. (2006), Nature, 443, 7113, 835-837.

Acknowledgments: Authors are thankful to Space Application Center (SAC), Ahmedabad, India, for providing fund and MiniSAR data to carry out this research work.

Table 1. Result of electrical properties measured for both regions

Property	Region 1	Region 2
ε'	3.26	3.41
ε''	0.026	0.032
tanδ	0.0073	0.0079
$\rho (g/cm^3)$	1.77	1.83

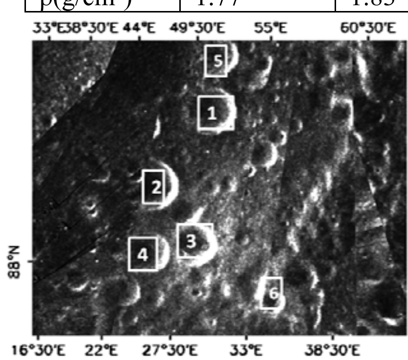

Fig. 1 S_1 image showing selected region of interest (ROI) areas on MINISAR data of Peary crater

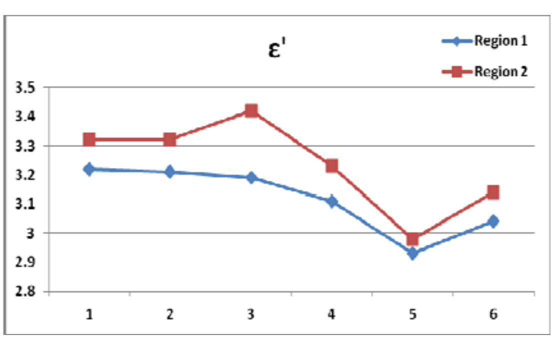

Fig. 2 Real part of dielectric constant of both the regions for selected ROIs.

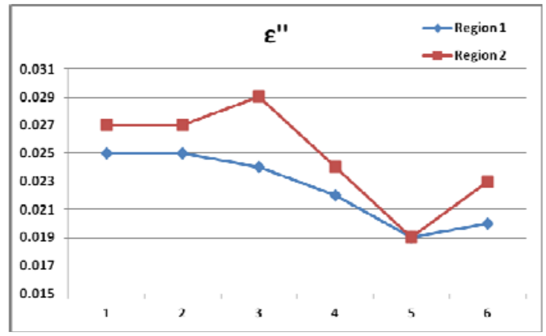

Fig. 3 Imaginary part of dielectric constant of both the regions for selected ROIs.

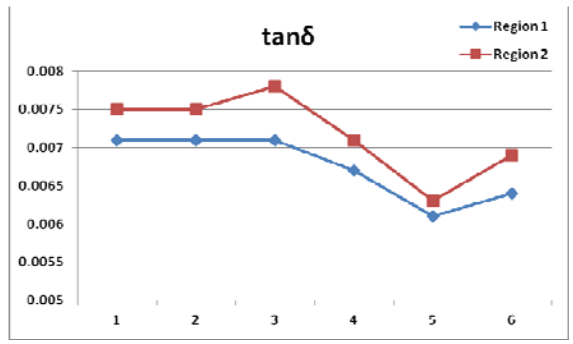

Fig. 4 Loss tangent of both the regions for selected ROIs.

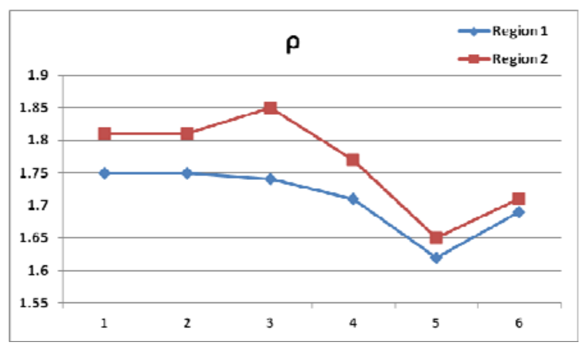

Fig. 5 Regolith density of both the regions for selected ROIs.